Superexchange Liquefaction of Strongly Correlated Lattice Dipolar Bosons

Ivan Morera,[1,2] Rafał Ołdziejewski,[3,4,*] Grigori E. Astrakharchik,[5,1,2] and Bruno Juliá-Díaz[1,2]
[1]Departament de Física Quàntica i Astrofísica, Facultat de Física, Universitat de Barcelona, E-08028 Barcelona, Spain
[2]Institut de Ciències del Cosmos, Universitat de Barcelona, ICCUB, Martí i Franquès 1, E-08028 Barcelona, Spain
[3]Max Planck Institute of Quantum Optics, 85748 Garching, Germany
[4]Munich Center for Quantum Science and Technology, Schellingstrasse 4, 80799 Munich, Germany
[5]Departament de Física, Universitat Politècnica de Catalunya, Campus Nord B4-B5, E-08034 Barcelona, Spain

(Received 15 April 2022; revised 3 November 2022; accepted 7 December 2022; published 12 January 2023)

We propose a mechanism for liquid formation in strongly correlated lattice systems. The mechanism is based on an interplay between long-range attraction and superexchange processes. As an example, we study dipolar bosons in one-dimensional optical lattices. We present a perturbative theory and validate it in comparison with full density-matrix renormalization group simulations for the energetic and structural properties of different phases of the system, i.e., self-bound Mott insulator, liquid, and gas. We analyze the nonequilibrium properties and calculate the dynamic structure factor. Its structure differs in compressible and insulating phases. In particular, the low-energy excitations in compressible phases are linear phonons. We extract the speed of sound and analyze its dependence on dipolar interaction and density. We show that it exhibits a nontrivial behavior owing to the breaking of Galilean invariance. We argue that an experimental detection of this previously unknown quantum liquid could provide a fingerprint of the superexchange process and open intriguing possibilities for investigating non-Galilean invariant liquids.

DOI: 10.1103/PhysRevLett.130.023602

Introduction.—Ultracold atoms in optical lattices might serve as a quantum simulator of the Hubbard model that plays a vital role in our understanding of strongly correlated solid-state materials [1]. Particularly, the Hubbard model at strong coupling displays superexchange processes which can be employed to simulate different quantum magnetic systems [2–6]. Moreover, the recent experimental progress with atoms possessing strong magnetic moments, like Dy, has led to the first realization of an extended Bose-Hubbard model (EBH) in 3D [7] and 1D [8]. The addition of a long-range potential to the interplay between on-site repulsion and periodic confinement holds promise for exciting new physics to emerge, e.g., quasilocalization [9,10] and unexpected topological phases [11,12].

The classical van der Waals theory of fluids states that self-bound liquids exist due to the attractive finite-range part of the interparticle interaction stabilized by the repulsive short-range core [13]. Recently, a novel paradigmatic quantum liquid has been observed in ultracold systems that is simultaneously ultradilute and coherent [14–21]. Contrary to the van der Waals mechanism, the weakly interacting quantum gases undergo liquefaction due to the zero-point energy fluctuations [22]—the so-called Lee-Huang-Yang term [23–25]. Notably, quantum liquids are even more robust in lower dimensions owing to an enhanced role of quantum fluctuations for both two-component and dipolar gases [26–34], while in classical systems the van der Waals mechanism cannot prevent a collapse of the classical system with long-range interactions in lower dimensions. Interestingly, microscopic foundations of quantum liquid formation for weakly interacting Bose-Bose mixtures can be studied in one-dimensional optical lattices [35,36].

In this Letter, we study an unconventional microscopic mechanism of liquid formation for a system confined to a one-dimensional optical lattice with strong on-site repulsion—in the vicinity of the Tonks-Girardeau (TG) limit—and long-range attraction. Notably, we show that the appearance of superexchange processes liquefies the gas state close to an insulator phase transition rendering a quantum droplet for moderate and large system sizes.

Setup and model.—We consider a one-dimensional system of ultracold dipolar bosons loaded to a deep optical lattice comprising N_s sites. The corresponding Hamiltonian is given by an extended Bose-Hubbard model,

$$\hat{H} = \sum_{i=1}^{N_s} \left[\frac{U}{2} \hat{n}_i(\hat{n}_i - 1) - J(\hat{b}_i^\dagger \hat{b}_{i+1} + \text{H.c.}) \right] + V \sum_{i<j}^{N_s} \frac{\hat{n}_i \hat{n}_j}{|i-j|^3}, \tag{1}$$

with hopping J, on-site interaction U, and dipolar strength V. Importantly, it is possible to tune U/J and V/J separately in experiments with 1D optical lattices [37], e.g., by using Feshbach resonances and adjusting the polarization angle of the magnetic moment in the system. Thus, all the phases considered should be accessible for future experiments with Dy or Er atoms similar to existing state-of-art settings [8,37]; see the Supplemental Material [38]. A typical transverse length of a trapping potential in current experiments with ultracold gases $\sigma_\perp \approx 50$ nm [37] is much smaller than a typical lattice spacing $a \approx 500$ nm. We thus use pure dipolar interaction in 1D instead of the effective potential for quasi-1D geometries, which includes corrections at distances of the order of $\sigma_\perp$ [51]. In the following, we study the ground state of the system described by Hamiltonian (1) for large values of the on-site repulsion ($U/J \gg 1$) by developing perturbation theory and performing numerical simulations.

Insulator instability.—We start by investigating an impenetrable lattice TG gas ($U/J \to \infty$) perturbed by an attractive dipolar interaction ($|V| \sim J$). We develop an analytical theory by assuming a lattice TG state $|\psi_{\mathrm{TG}}\rangle$ at a density $n = N/N_s$ and calculating the effective equation of state (EOS) perturbatively as $E = \langle\psi_{\mathrm{TG}}|\hat{H}|\psi_{\mathrm{TG}}\rangle$. The resulting energy per particle $e \equiv E/N$ reads $e = e_J + e_V$, where

$$e_J = -2J\sin(n\pi)/(n\pi),$$
$$e_V = V\left(\zeta(3)n - \frac{\zeta(5)}{2n\pi^2} + \frac{1}{4n\pi^2}[\mathrm{Li}_5(e^{2i\pi n}) + \mathrm{Li}_5(e^{-2i\pi n})]\right), \tag{2}$$

indicate the kinetic energy of the fermionized bosons and the dipolar interaction energy accordingly. We also introduce the polylogarithm function $\mathrm{Li}_\beta(n)$ of order β.

We classify the different phases of the system based on the value of the equilibrium density n_0, defined as the density at which the energy per particle is minimal. The gaseous (GAS) phase is characterized by a vanishing equilibrium density $n_0 = 0$ and it appears for $V < V_{\mathrm{BMI}}$ [52]. At the critical value $V = V_{\mathrm{BMI}}$, the minimum of the EOS jumps to unit density $n_0 = 1$ signaling a first-order transition to an insulator state. Furthermore, the insulator state has a lower energy per particle than the free particle energy $-2J$. It is thus a self-bound state, to which we refer to as a self-bound Mott insulator (BMI). The threshold of the BMI state is defined by the condition that the energy per particle at unit filling equals the free energy per particle $e(n = 1) = -2J$, giving the critical value of the long-range interaction $V_{\mathrm{BMI}}/J = -2/\zeta(3)$. BMI states are incompressible. Thus in finite systems they become completely localized exhibiting compact density profiles with a saturated density corresponding to strictly one particle per site $n = 1$ (see Fig. 3). Although the density profile for these states bears similarity to quantum droplets, quantum correlations are completely suppressed in the BMI case (see Fig. 3). Therefore, one should not consider them as genuine liquids. In fact, they can be related to phase-separated states in spin systems [53].

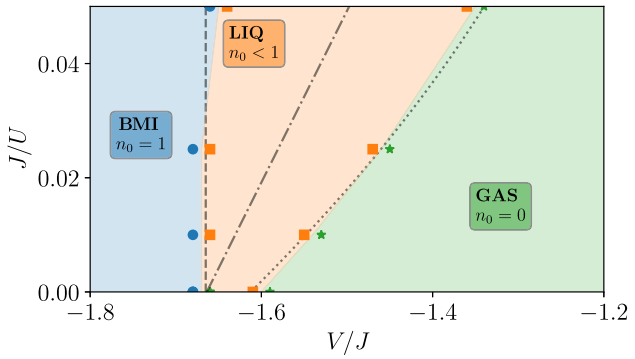

FIG. 1. Phase diagram for dipolar bosons in a one-dimensional optical lattice. Different phases can be characterized by their respective equilibrium densities n_0. We encounter a gaseous phase (GAS), a liquid one (LIQ), and a self-bound Mott-insulator (BMI). Dashed and dot-dashed lines denote, respectively, LIQ-to-BMI and GAS-to-LIQ transitions obtained in perturbation theory. The dotted line indicates the threshold for a bound state (dimer) in the two-body problem.

Importantly, lattice physics significantly differs from what one expects to find in a continuous analog of the described system. In the 1D continuum, the addition of attractive dipolar interaction to TG gas leads to the collapse of the system as the quantum fluctuations cannot compensate for the diverging dipolar attraction. The feature of a lattice is that it provides a natural regularization of the problem since, for hard-core particles, the maximum density allowed is fixed by the lattice spacing ($n \leq 1$). Note, however, that genuine self-bound droplets in the TG limit for quasi-1D dipolar bosons, where the existence of transverse structure regularizes short-range divergence, were predicted recently [32].

Superexchange processes and liquefaction.—The mechanism lying behind BMI formation is based on a near cancellation between the effective repulsion coming from the kinetic energy of lattice hard-core particles and the long-range dipolar attraction. In the following, we study the effects of relaxing the hard-core condition in our system.

We consider penetrable bosons with large but finite on-site interaction $U/J \gg 1$. We thus move away from the TG limit that opens the possibility of next-to-nearest neighbor hopping through a virtual intermediate process of two bosons occupying the same site—the so-called superexchange process. Explicitly, this extra contribution e_U to the total energy e can be derived using the effective fermionic Hamiltonian within the second-order degenerate perturbation theory [38,39], and it reads:

$$e_U = -\frac{4J^2}{U}n\left(1 - \frac{\sin(2\pi n)}{2\pi n}\right). \tag{3}$$

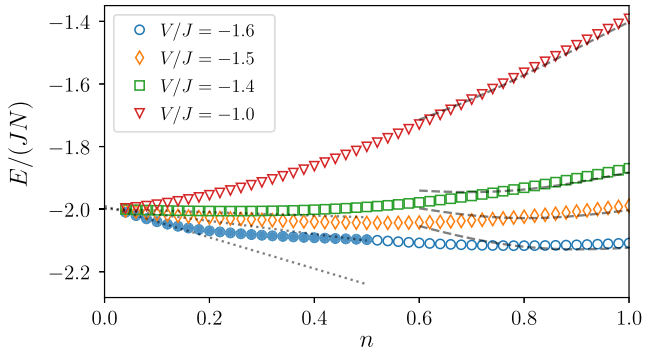

FIG. 2. Equation of state of dipolar bosons in a one-dimensional optical lattice for different dipolar strength V/J and fixed on-site repulsion $U/J = 20$. Filled symbols denote inhomogeneous solutions. Dashed lines show the Tonks-Girardeau perturbative result [38]. The dotted line shows the behavior expected for a lattice soliton solution [54]. Liquid forms when the equation of state shows a minimum at some finite value of density n_0 with the energy per particle $E/(N_s n_0) < -2J$; see $V/J = -1.4, -1.5, -1.6$ curves. A gas occurs when the minimum is located at zero density with the energy per particle $E/N > -2J$; see the $V/J = -1.0$ curve.

Note that the superexchange correction effectively introduces additional attraction of order $J^2/U \ll 1$ in the system for all densities.

Remarkably, by inspecting the modified EOS of the ground state, we encounter a gas-to-liquid transition close to the BMI boundary owing entirely to the emerging superexchange process, which diminishes on-site repulsion; see Fig. 1. The found liquid phase is characterized by a negative energy per particle smaller than for the free case $E/N < -2J$ and a finite equilibrium density $0 < n_0 < 1$ (see Fig. 2). By increasing the attractive long-range coupling, the density saturates with one particle per site, and consequently, the system enters the BMI state.

Notably, the discovered mechanism of liquefaction in the strongly correlated regime bears certain similarities with the one vastly studied in the opposite limit of weak interactions. As therein, quantum liquids appear due to the subleading terms when dominating contributions of opposite signs cancel each other [22]. Nonetheless, contrary to the Lee-Huang-Yang term as a small beyond mean-field effect, the superexchange correlations occur for strongly interacting systems well beyond the mean-field applicability.

Equilibrium properties.—To benchmark the perturbative EOS, we calculate the ground-state energy of Hamiltonian (1) using the density-matrix renormalization group (DMRG) algorithm; see Ref. [38]. We compute the ground state for different strengths of the long-range interaction V/J keeping fixed a large but finite on-site interaction U/J; see Fig. 2. In the case of larger densities ($n \gtrsim 0.8$), an excellent agreement is found for any value of the long-range interaction, especially when approaching the unit filling limit $n = 1$ owing to suppressed quantum correlations. For smaller densities ($n \lesssim 0.5$), the effective EOS deviates significantly, as it does not include the presence of few-body bound states. In DMRG simulations, we always observe that the appearance of the liquid phase coincides with the formation of a two-body bound state in the system; see Fig. 1. Details on solving the two-body problem are given in Ref. [38]. In the few-body limit, the equation of state is well approximated by a lattice soliton solution [54] $(E/N) + 2J \sim [(N-1)/2]\epsilon_b$, with ϵ_b being the two-particle bound-state energy; see Fig. 2.

The EOS allows one to differentiate three distinct phases in the system; see Fig. 2. The gaseous phase features a minimum in the EOS at zero density $n_0 = 0$ and a positive energy per particle compared to the free case $e > -2J$. On the other hand, the liquid and BMI phases are characterized by negative binding energies $e < -2J$ in the minimum. The equilibrium density of a liquid ranges within $0 < n_0 < 1$, and saturates to $n_0 = 1$ in the BMI phase, making its EOS singular. Moreover, the liquid state is compressible while the BMI is not.

One of the qualitative differences between the predictions of perturbative theory and DMRG results is the presence of a narrow liquid phase in the TG limit $J/U = 0$. This liquid state is sandwiched between the gas and BMI phases for $V_{\mathrm{MI}} < V < -1.61J$; see Fig. 1. The weakest attraction, for which the liquid forms, is defined by the existence of a two-body bound state. Remarkably, for the dipolar interaction, the formation of a two-body bound state does not coincide with the formation of a self-bound MI state in the many-body problem for $J/U = 0$, in contrast to faster decaying potentials. We thus relate the presence of the liquid phase to the long-range nature of the dipolar interaction.

The equilibrium properties differ dramatically among the various phases, as shown in Fig. 3. The equilibrium density ranges from $0 < n_0 < 1$ in the liquid phase and saturates to $n_0 = 1$ in the BMI phase. DMRG simulations result in density profiles that do not fill the entire lattice for these phases, contrary to the gaseous state; see inset of Fig. 3. Moreover, the value of the saturated density agrees excellently with the equilibrium density found from the EOS. Its value increases almost linearly for the growing attractive long-range interaction in the liquid phase. Upon reaching the BMI phase, the equilibrium density saturates to $n_0 = 1$ and becomes independent of the dipolar coupling.

Another important observable pertains to the particle variance $\Delta n_0 = \sqrt{\langle\langle \hat{n}_0^2 \rangle - n_0^2\rangle}$, as it quantifies the fluctuations of density and probes the structure of pair correlations. Particularly, it vanishes in the gas phase (due to vanishing equilibrium density) and in the BMI phase becomes of order $J/\sqrt{U}$. We find that the maximal value of Δn is reached in the liquid phase close to half filling, $n_0 \sim 1/2$. Fascinatingly, the lattice TG model captures the particle variance model well and provides a precise analytic description; see Fig. 3.

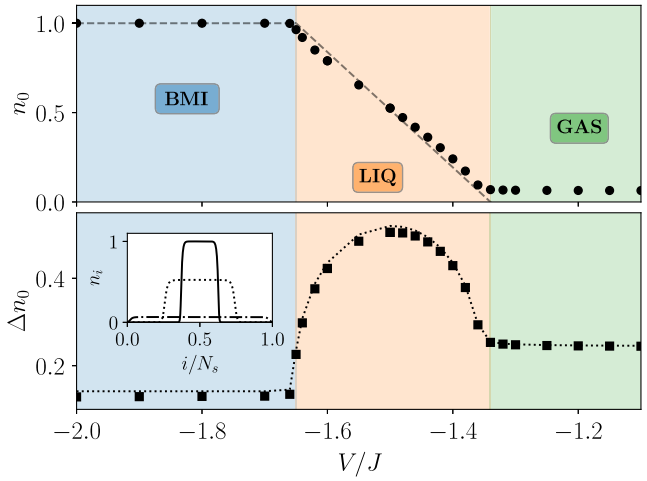

FIG. 3. Density and its variance as a function of V/J for a fixed $U/J = 20$. Top: saturated density n_0 (circles). Dashed line: unit filling, $n_0 = 1$ (BMI); zero filling, $n_0 = 0$ (GAS); linear interpolation (LIQ). We have performed open boundary conditions numerical simulations up to a density $n = 50/800$. Bottom: particle number variance $\Delta n_0^2 = \langle \hat{n}_0^2 \rangle - \langle \hat{n}_0 \rangle^2$ (squares). The dotted line denotes the particle number variance obtained in a TG-like state; see the main text. Inset: characteristic density profiles obtained for $V/J = -1.8$ (BMI), $V/J = -1.5$ (LIQ), and $V/J = -1.3$ (GAS).

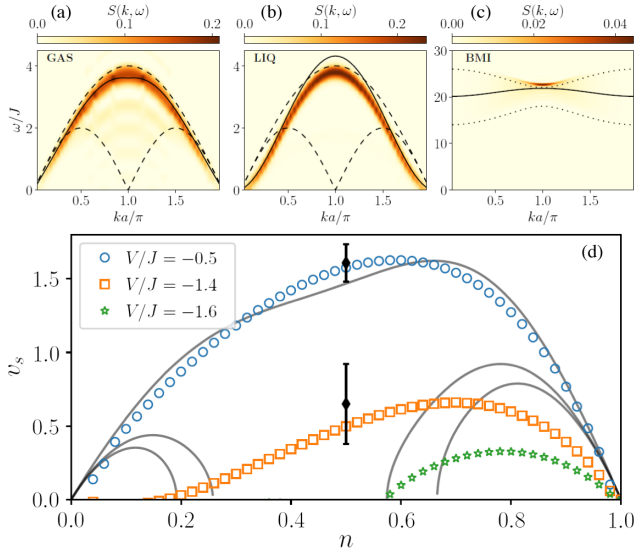

FIG. 4. (a)–(c) Dynamic structure factor for (a) the GAS phase ($V/J = -0.5$, $U/J = 20$, and $n = 25/50$), (b) the LIQ phase ($V/J = -1.4$, $U/J = 20$, and $n = 25/50$), and (c) the BMI phase ($V/J = -1.4$, $U/J = 20$, and $n = 50/50$). Upper and lower bounds to the excitation energies for $V/J = 0$ are obtained from Bethe ansatz [40,57] (dashed lines) for GAS and LIQ and from first-order perturbation theory [41–43,49] (dotted lines) for BMI. (d) Speed of sound as a function of the density for different values of V/J and a fixed $U/J = 20$. Symbols from lattice Feynman relation (see the main text), lines from perturbative results, and black diamonds extracted from the dynamic structure factor.

Nonequilibrium properties.—As nonequilibrium properties can be experimentally measured [55,56], we investigate the dynamic structure factor $S(k, \omega)$. It quantifies the structure and strength of the two-particle excitations allowing an additional verification of the phases. In Figs. 4(a)–4(c), we provide characteristic examples of $S(k, \omega)$ in different phases. The structure of the excitations differs drastically whether the system is compressible or not. A single mode exhausts the spectrum in the GAS and LIQ phases. Indeed, the position of the peak in $S(k, \omega)$ is close to the prediction of the Feynman relation, $\omega(k) = [\langle \hat{b}_i^\dagger \hat{b}_{i+1} \rangle \epsilon(k)/nS(k)]$, derived in the single-mode approximation. Such behavior profoundly varies from that of a spinonlike spectrum expected at half filling [40,57], in which modes are populated from the lower (one-particle or -hole excitation) up to upper (two-particle excitation) branches; see dashed lines in Figs. 4(a) and 4(b). The presence of dipolar interactions strongly affects the excitations, creating a dominant mode located close to the upper branch. Such a behavior is typical of systems that are softer than the TG gas and possess larger values of the Luttinger parameter, $K > 1$ [58]. We verify that the lowest-energy modes in compressible phases are linear phonons, validating the applicability of the Luttinger liquid theory. By employing a flattop model, i.e., $S(k, \omega) = \text{const}$, $\omega_-(k) < \omega < \omega_+(k)$ (see SM for details [38]), we demonstrate that the spectral weight diverges $S(k, v_s k) \propto 1/k^2$ as $k \to 0$, that is, the phonon mode is greatly populated, in agreement with the numerical simulations. The structure of excitations differs dramatically in the BMI phase, wherein a gap Δ opens. From the flattop model analysis, we infer that the spectral weight vanishes at small momenta, $S(k, \Delta) \propto k^2$ for $k \to 0$. Instead, the edge of the Brillouin zone, $k_{\mathrm{BZ}} = \pi/a$, gets strongly populated, and a sharp peak is formed in $S(k_{\mathrm{BZ}}, \omega)$ so that the lattice Feynman relation captures well the value of the gap. In absence of dipolar interactions, the upper and lower bounds are no longer given by one- or two-particle excitations but rather by doublon-holon excitations, shown with dotted lines.

Having studied the dynamic structure factor in the three phases, we focus now on the speed of sound. The presence of a lattice has strong consequences on sound propagation [59,60] and other transport properties [61], as can be traced to the loss of Galilean invariance in the lattice. This produces a nontrivial dependence of the sound on the density. To obtain the speed of sound v_s, we calculate static structure factor $S(k)$, compute the compressibility κ_s from the EOS, and employ the non-Galilean version of the Feynman relation [38,62], $S(k) = \kappa_s v_s nk/2$ applicable for small momenta. In Fig. 4(d), we present the sound velocity as a function of the density for different values of the long-range coupling. For weak dipolar attraction, the speed of sound decreases above half filling and reaches zero at unit filling, signaling the transition to a MI state. As the dipolar strength increases, a liquid state forms, and the sound velocity also vanishes at spinodal density $n_s \leq 1$. Finally,

when approaching the BMI phase, the sound velocity nears zero for any value of density showing no stable homogeneous solution exists for $|V| > |V_{\mathrm{BMI}}|$.

For an analytical estimation of the speed of sound, we employ the non-Galilean invariant Luttinger liquid theory [38,59,60]. For weak dipolar attraction, we note an agreement between the perturbative theory and exact numerical analysis. For the increased strength of attraction, the analytical approach predicts the appearance of a spinodal point, albeit at an incorrect density value. Additionally, we report a qualitative difference at small densities where perturbative theory predicts a finite value of the speed of sound, in stark contrast with numerical results where no stable homogeneous solution exists for $n \leq n_s$. We associate this discrepancy with the formation of molecules at small densities, which is overlooked in the perturbative description.

Discussion and outlook.—Our Letter shows an unconventional mechanism for liquid formation in strongly correlated lattice systems. Specifically, liquefaction arises due to an interplay between nonlocal attraction and the superexchange processes originating from short-range repulsion. Our Letter presents a nontrivial extension of the quantum van der Waals theory to lattice systems. Our predictions apply to lattice systems described by one-dimensional EBH Hamiltonians. These could be realized experimentally in different ultracold atomic platforms like dipolar bosons [8,37], Rydberg atoms [63,64], or even excitonic systems [65]. Recently, one-dimensional dipolar bosonic systems were produced experimentally [37] and loaded into corresponding optical lattices [8].

This work has been funded by Grants No. PID2020–114626 GB-I00 and No. PID2020–113565 GB-C21 from the MICIN/AEI/10.13039/501100011033 and by the Ministerio de Economia, Industria y Competitividad (MINECO, Spain) under Grants No. FIS2017-84114-C2-1-P and No. FIS2017-87534-P. We acknowledge financial support from Secretaria d'Universitats i Recerca del Departament d'Empresa i Coneixement de la Generalitat de Catalunya, cofunded by the European Union Regional Development Fund within the ERDF Operational Program of Catalunya (project QuantumCat, Ref. No. 001-P001644). R. O. acknowledges support by the Max Planck Society and the Deutsche Forschungsgemeinschaft (DFG, German Research Foundation) under Germany's Excellence Strategy–EXC-2111–390814868.

*Corresponding author.
rafal.oldziejewski@mpq.mpg.de

[1] M. Lewenstein, A. Sanpera, and V. Ahufinger, *Ultracold Atoms in Optical Lattices* (Oxford University Press, New York, 2012).
[2] L.-M. Duan, E. Demler, and M. D. Lukin, Phys. Rev. Lett. **91**, 090402 (2003).
[3] S. Trotzky, P. Cheinet, S. Fölling, M. Feld, U. Schnorrberger, A. M. Rey, A. Polkovnikov, E. A. Demler, M. D. Lukin, and I. Bloch, Science **319**, 295 (2008).
[4] L.-M. Duan, E. Demler, and M. D. Lukin, Phys. Rev. Lett. **91**, 090402 (2003).
[5] T. Fukuhara, A. Kantian, M. Endres, M. Cheneau, P. Schauß, S. Hild, D. Bellem, U. Schollwöck, T. Giamarchi, C. Gross, I. Bloch, and S. Kuhr, Nat. Phys. **9**, 235 (2013).
[6] P. N. Jepsen, J. Amato-Grill, I. Dimitrova, W. W. Ho, E. Demler, and W. Ketterle, Nature (London) **588**, 403 (2020).
[7] S. Baier, M. J. Mark, D. Petter, K. Aikawa, L. Chomaz, Z. Cai, M. Baranov, P. Zoller, and F. Ferlaino, Science **352**, 201 (2016).
[8] G. Natale, T. Bland, S. Gschwendtner, L. Lafforgue, D. S. Grün, A. Patscheider, M. J. Mark, and F. Ferlaino, arXiv:2205.03280.
[9] L. Barbiero, C. Menotti, A. Recati, and L. Santos, Phys. Rev. B **92**, 180406(R) (2015).
[10] W. Li, A. Dhar, X. Deng, K. Kasamatsu, L. Barbiero, and L. Santos, Phys. Rev. Lett. **124**, 010404 (2020).
[11] R. Kraus, T. Chanda, J. Zakrzewski, and G. Morigi, Phys. Rev. B **106**, 035144 (2022).
[12] J. Fraxanet, D. González-Cuadra, T. Pfau, M. Lewenstein, T. Langen, and L. Barbiero, Phys. Rev. Lett. **128**, 043402 (2022).
[13] J. D. Van Der Waals and J. S. Rowlinson, *On the Continuity of the Gaseous and Liquid States* (Dover Publications, Mineola, 2004).
[14] M. Schmitt, M. Wenzel, F. Böttcher, I. Ferrier-Barbut, and T. Pfau, Nature (London) **539**, 259 (2016).
[15] I. Ferrier-Barbut, H. Kadau, M. Schmitt, M. Wenzel, and T. Pfau, Phys. Rev. Lett. **116**, 215301 (2016).
[16] L. Chomaz, S. Baier, D. Petter, M. J. Mark, F. Wächtler, L. Santos, and F. Ferlaino, Phys. Rev. X **6**, 041039 (2016).
[17] I. Ferrier-Barbut, M. Wenzel, F. Böttcher, T. Langen, M. Isoard, S. Stringari, and T. Pfau, Phys. Rev. Lett. **120**, 160402 (2018).
[18] F. Böttcher, M. Wenzel, J.-N. Schmidt, M. Guo, T. Langen, I. Ferrier-Barbut, T. Pfau, R. Bombín, J. Sánchez-Baena, J. Boronat, and F. Mazzanti, Phys. Rev. Res. **1**, 033088 (2019).
[19] C. R. Cabrera, L. Tanzi, J. Sanz, B. Naylor, P. Thomas, P. Cheiney, and L. Tarruell, Science **359**, 301 (2018).
[20] P. Cheiney, C. R. Cabrera, J. Sanz, B. Naylor, L. Tanzi, and L. Tarruell, Phys. Rev. Lett. **120**, 135301 (2018).
[21] G. Semeghini, G. Ferioli, L. Masi, C. Mazzinghi, L. Wolswijk, F. Minardi, M. Modugno, G. Modugno, M. Inguscio, and M. Fattori, Phys. Rev. Lett. **120**, 235301 (2018).
[22] D. S. Petrov, Phys. Rev. Lett. **115**, 155302 (2015).
[23] T. D. Lee, K. Huang, and C. N. Yang, Phys. Rev. **106**, 1135 (1957).
[24] A. R. P. Lima and A. Pelster, Phys. Rev. A **84**, 041604(R) (2011).
[25] A. R. P. Lima and A. Pelster, Phys. Rev. A **86**, 063609 (2012).
[26] D. S. Petrov and G. E. Astrakharchik, Phys. Rev. Lett. **117**, 100401 (2016).
[27] D. Edler, C. Mishra, F. Wächtler, R. Nath, S. Sinha, and L. Santos, Phys. Rev. Lett. **119**, 050403 (2017).

[28] G. E. Astrakharchik and B. A. Malomed, Phys. Rev. A **98**, 013631 (2018).
[29] P. Zin, M. Pylak, T. Wasak, M. Gajda, and Z. Idziaszek, Phys. Rev. A **98**, 051603(R) (2018).
[30] T. Ilg, J. Kumlin, L. Santos, D. S. Petrov, and H. P. Büchler, Phys. Rev. A **98**, 051604(R) (2018).
[31] D. Rakshit, T. Karpiuk, P. Zin, M. Brewczyk, M. Lewenstein, and M. Gajda, New J. Phys. **21**, 073027 (2019).
[32] R. Ołdziejewski, W. Górecki, K. Pawłowski, and K. Rzążewski, Phys. Rev. Lett. **124**, 090401 (2020).
[33] S. De Palo, E. Orignac, and R. Citro, Phys. Rev. B **106**, 014503 (2022).
[34] G. Guijarro, G. E. Astrakharchik, and J. Boronat, Phys. Rev. Lett. **128**, 063401 (2022).
[35] I. Morera, G. E. Astrakharchik, A. Polls, and B. Juliá-Díaz, Phys. Rev. Res. **2**, 022008(R) (2020).
[36] I. Morera, G. E. Astrakharchik, A. Polls, and B. Juliá-Díaz, Phys. Rev. Lett. **126**, 023001 (2021).
[37] W. Kao, K.-Y. Li, K.-Y. Lin, S. Gopalakrishnan, and B. L. Lev, Science **371**, 296 (2021).
[38] See Supplemental Material at http://link.aps.org/supplemental/10.1103/PhysRevLett.130.023602 for additional information on perturbation theory, two-body bound state formation, numerical methods, calculation of the sound velocity in a lattice, calculation of the dynamic structure factor, and experimental implementation of the model, which includes Refs. [39–49].
[39] M. A. Cazalilla, Phys. Rev. A **67**, 053606 (2003).
[40] T. Yamada, Prog. Theor. Phys. **41**, 880 (1969).
[41] A. Iucci, M. A. Cazalilla, A. F. Ho, and T. Giamarchi, Phys. Rev. A **73**, 041608(R) (2006).
[42] A. Tokuno and T. Giamarchi, Phys. Rev. Lett. **106**, 205301 (2011).
[43] S. Ejima, H. Fehske, and F. Gebhard, J. Phys. **391**, 012143 (2012).
[44] B. Pirvu, V. Murg, J. I. Cirac, and F. Verstraete, New J. Phys. **12**, 025012 (2010).
[45] J. Haegeman, J. I. Cirac, T. J. Osborne, I. Pižorn, H. Verschelde, and F. Verstraete, Phys. Rev. Lett. **107**, 070601 (2011).
[46] J. Haegeman, C. Lubich, I. Oseledets, B. Vandereycken, and F. Verstraete, Phys. Rev. B **94**, 165116 (2016).
[47] T. Barthel, U. Schollwöck, and S. R. White, Phys. Rev. B **79**, 245101 (2009).
[48] R. Roth and K. Burnett, J. Phys. B **37**, 3893 (2004).
[49] S. Ejima, H. Fehske, F. Gebhard, K. zu Münster, M. Knap, E. Arrigoni, and W. von der Linden, Phys. Rev. A **85**, 053644 (2012).
[50] R. G. Pereira, S. R. White, and I. Affleck, Phys. Rev. Lett. **100**, 027206 (2008).
[51] F. Deuretzbacher, J. C. Cremon, and S. M. Reimann, Phys. Rev. A **81**, 063616 (2010).
[52] Note that the vanishing equilibrium density ($n_0 = 0$) in the gas phase can be reached only in the $N_s \to \infty$ limit. Instead, in a finite size system, the gas always stays at some finite pressure. However, zero pressure can be found in finite systems for self-bound states (LIQ and BMI) with an equilibrium density n_0.
[53] D. Petrosyan, B. Schmidt, J. R. Anglin, and M. Fleischhauer, Phys. Rev. A **76**, 033606 (2007).
[54] A. Scott, J. Eilbeck, and H. Gilhøj, Physica (Amsterdam) **78D**, 194 (1994).
[55] R. Landig, F. Brennecke, R. Mottl, T. Donner, and T. Esslinger, Nat. Commun. **6**, 7046 (2015).
[56] M. Cheneau, P. Barmettler, D. Poletti, M. Endres, P. Schauß, T. Fukuhara, C. Gross, I. Bloch, C. Kollath, and S. Kuhr, Nature (London) **481**, 484 (2012).
[57] J. des Cloizeaux and J. J. Pearson, Phys. Rev. **128**, 2131 (1962).
[58] J.-S. Caux and P. Calabrese, Phys. Rev. A **74**, 031605(R) (2006).
[59] M. A. Cazalilla, J. Phys. B **37**, S1 (2004).
[60] M. A. Cazalilla, Phys. Rev. A **70**, 041604(R) (2004).
[61] R. Anderson, F. Wang, P. Xu, V. Venu, S. Trotzky, F. Chevy, and J. H. Thywissen, Phys. Rev. Lett. **122**, 153602 (2019).
[62] K. V. Krutitsky, Phys. Rep. **607**, 1 (2016).
[63] H. Labuhn, D. Barredo, S. Ravets, S. de Léséleuc, T. Macrì, T. Lahaye, and A. Browaeys, Nature (London) **534**, 667 (2016).
[64] A. Browaeys and T. Lahaye, Nat. Phys. **16**, 132 (2020).
[65] C. Lagoin, U. Bhattacharya, T. Grass, R. W. Chhajlany, T. Salamon, K. Baldwin, L. Pfeiffer, M. Lewenstein, M. Holzmann, and F. Dubin, Nature (London) **609**, 485 (2022).